Supporting Information

Neurogenic and Angiogenic poly(N-Acryloylglycine)-co-(acrylamide)-co-(N-acryloyl-glutamate) Hydrogel: Preconditioning Effect Under Oxidative Stress and use in neuroregeneration

Kirti Wasnik[a], Prem Shankar Gupta[a], Gurmeet Singh[a], Somedutta Maity [b], Sukanya Patra [a], Divya Pareek [a], Sandeep Kumar[c], Vipin Rai[d†], Ravi Prakash[e], Arbind Acharya [c], Pralay Maiti[e], Sudip Mukherjee[a], Yitzhak Mastai[f], Pradip Paik[a *]

[a] School of Biomedical Engineering, Indian Institute of Technology, Banaras Hindu University (BHU), Varanasi, Uttar Pradesh 221 005, India

[b] School of Engineering Sciences and Technology, University of Hyderabad, Telangana State 500 046, India

[c] Department of Zoology, Banaras Hindu University (BHU), Varanasi, Uttar Pradesh 221 005, India

[d] Department of Biochemistry, Institute of Sciences, Banaras Hindu University (BHU), Varanasi, Uttar Pradesh 221 005, India

[e] School of Material Science, Indian Institute of Technology, Banaras Hindu University (BHU), Varanasi, Uttar Pradesh 221 005, India

[f] Department of Chemistry and the Institute of Nanotechnology, Bar-Ilan University, Ramat-Gan, 52900, Israel

ASSOCIATED CONTENT

Supporting Information

The supporting information contains, Figure S1. (a) FTIR spectra of N-acryloylglycine, (b) N-acryloylglutamic acid, (c) poly[(N-acryloylglycine)-b-(acrylamide)] (d) poly (N-acryloylglycine)-co-(acrylamide)-co-(N-acryloylglutamate) polymeric hydrogel; Figure S2. (A) ^{1}H NMR of N-acryloylglutamate monomer and (B) ^{13}C NMR of N-acryloylglycine monomer; Figure S3. (A) H1 NMR of p(NAG-Ac-NAE) hydrogel and (B) ^{13}C NMR of p(NAG-Ac-NAE) nanohydrogel.; Figure S4. (a) TGA and (b) DSC of the poly (N-acryloylglycine)-co-(acrylamide)-co-(N-acryloylglutamate) hydrogel; Figure S5. Shows the MALDI-TOF spectrum of p(NAG-Ac-NAE) hydrogel; Figure S6. Biodegradation behaviour of [p(NAG-Ac-NAE)] without replacing media, studied in PBS (pH 7.4) and in presence of different enzymes.; Figure S7. Size distribution and zeta potential of p(NAG-Ac-NAE) hydrogel, studied in PBS (pH 7.4), Figure S8. Cell viability of HUVEC in treatment of p(NAG-b-A) Figure S9. Anti-angiogenic property of p(NAG-b-A) hydrogel. (a) Vessel area (%) vs Time, (b) Total number of junctions (%) vs Time, (c) Junction density (%) vs time and (d) Total Vessel length (%) vs time. List of abbreviations is provided in supporting file.

Supporting Information

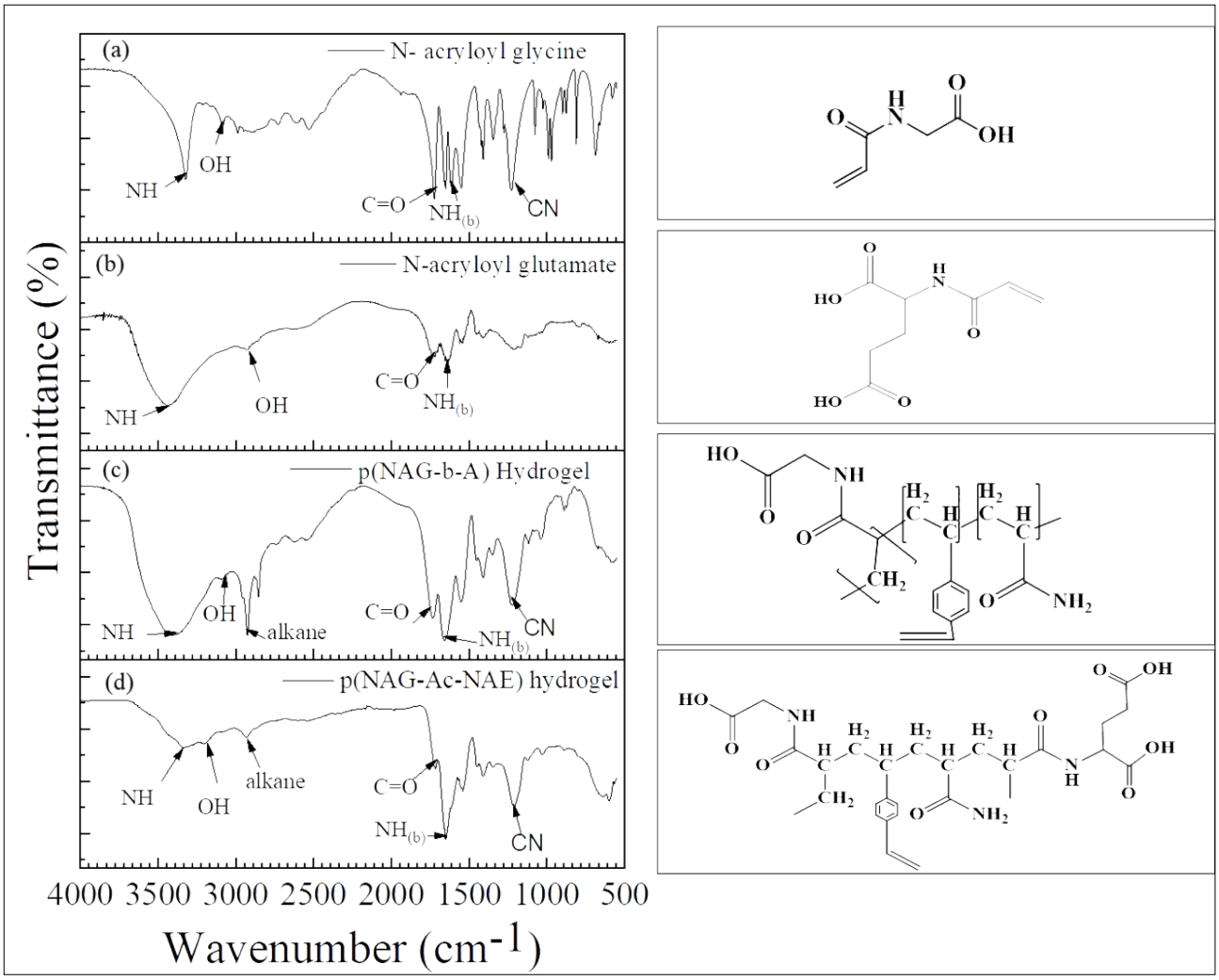

Figure S1. (a) FTIR spectra of N-acryloylglycine, (b) N-acryloylglutamic acid, (c) poly [(N-acryloylglycine)-b-(acrylamide)] (d) poly(N-acryloylglycine)-co-(acrylamide)-co-(N-acryloylglutamate) co-polymeric hydrogel.

For N- acryloylglycine**,** FTIR performed with KBr (Figure S1(a)): 3323 cm^{-1} (N-H (stretching), 3092 cm^{-1} (-O-H stretching), 1716 cm^{-1} (C=O (carbonyl) stretching), 1549 cm^{-1} (-O-H overtone), 1653 cm^{-1} (1^{st} overtone of ─NH), 1613 cm^{-1} (C=C α,β-unsaturated ketone and due to the presence of of amine).

Fig. S1(b): N- acryloylglutamaic FTIR performed in KBr: 3413 cm^{-1} (N-H (stretching)), 2912 cm^{-1} and 1408 cm^{-1} (─O─H stretching(hump); bending carboxylic acid), 1716 cm^{-1} (C=O (carbonyl) stretching),

1549 cm^{-1} (-O-H overtone), 1626 cm^{-1} (─NH_2), 1613 cm^{-1} (C=C α, β-unsaturated ketone, and due to the presence of amine).

Fig. S1(c): poly [(N-acryloyl glycine)-co-(acrylamide)-co-(N-acryloylglutamate)] nanohydrogel (p(NAG-Ac-NAE)) functional group analysis was performed through the ATR method: 3336 cm^{-1} (N─H (stretching)), 3182 cm^{-1} (─O─H stretching; strong broad carboxylic acid), 2912 (C─H stretching, conform the formation of polymer chain chain) 1716 cm^{-1} (–C═O (carbonyl) stretching), 1549 cm^{-1} (─O─H overtone), 1653 cm^{-1} (1^{st} overtone of ─NH).

FTIR results of poly(N-Acryloylglycine)-co-(acrylamide)-co-(N-acryloylglutamate) hydrogel has been discussed in the main texts of the manuscript

Supporting Information

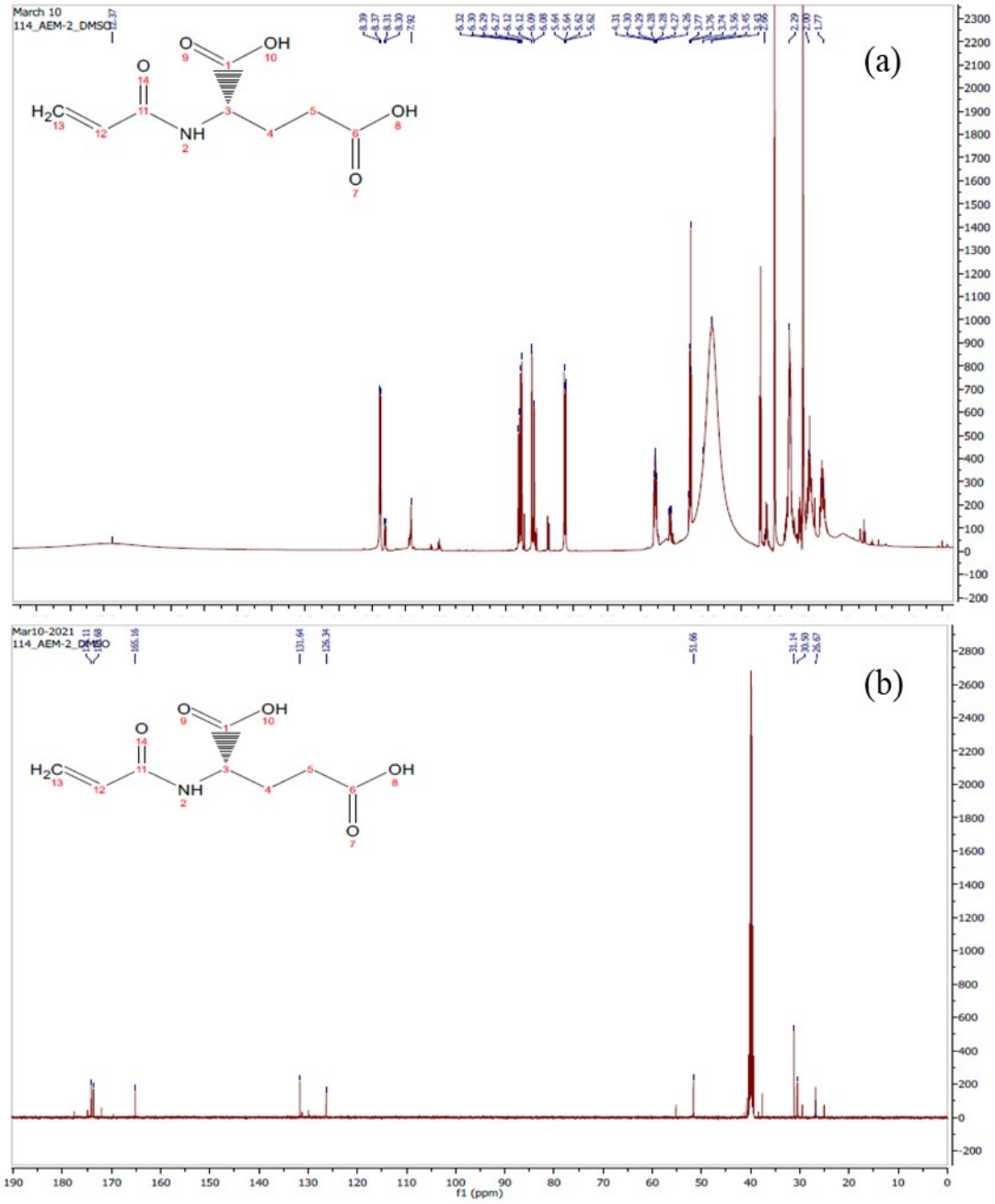

Figure S2. (A) ^{1}H NMR of N-acryloylglutamate monomer and (B) ^{13}C NMR of N-acryloylglycine monomer

^{1}H NMR spectrum chemical shifts (in ppm) (Fig. S2(a)): 12.5 δ (O─H of carboxylic acid (8^{th} and 12^{th} position)), 8.37 δ (N─H of 2° amines (2)), 6.13 δ (═C─H_2(13)), 6.13 δ (cis) and 5.64 δ (trans) of

($H_2C{=}CH_2$ (13 and 12)), 6.17 (─CH (12)), 4.29 δ (─CH (3)), 1.99 δ (─C─H_2 (4a and 4b)), 2.20 δ (─C─H_2 (5a and 5b)) 3.4 δ for H_2O and 2.5 for DMSO-d_6.

^{13}C NMR (500MHz, DMSO-d_6) (Figure S2 (b)): 174 and 173 ppm (─COOH (1 and 6)), 165 ppm (O═C─NH-R (11)), 126 ppm and 132ppm (C═C (13 and 12)) and 51.66 ppm (─CH (3)), 26.67 ppm 31.14 ppm (─CH_2─CH_2 (4 and 5)) 40 ppm band of DMSO-d_6

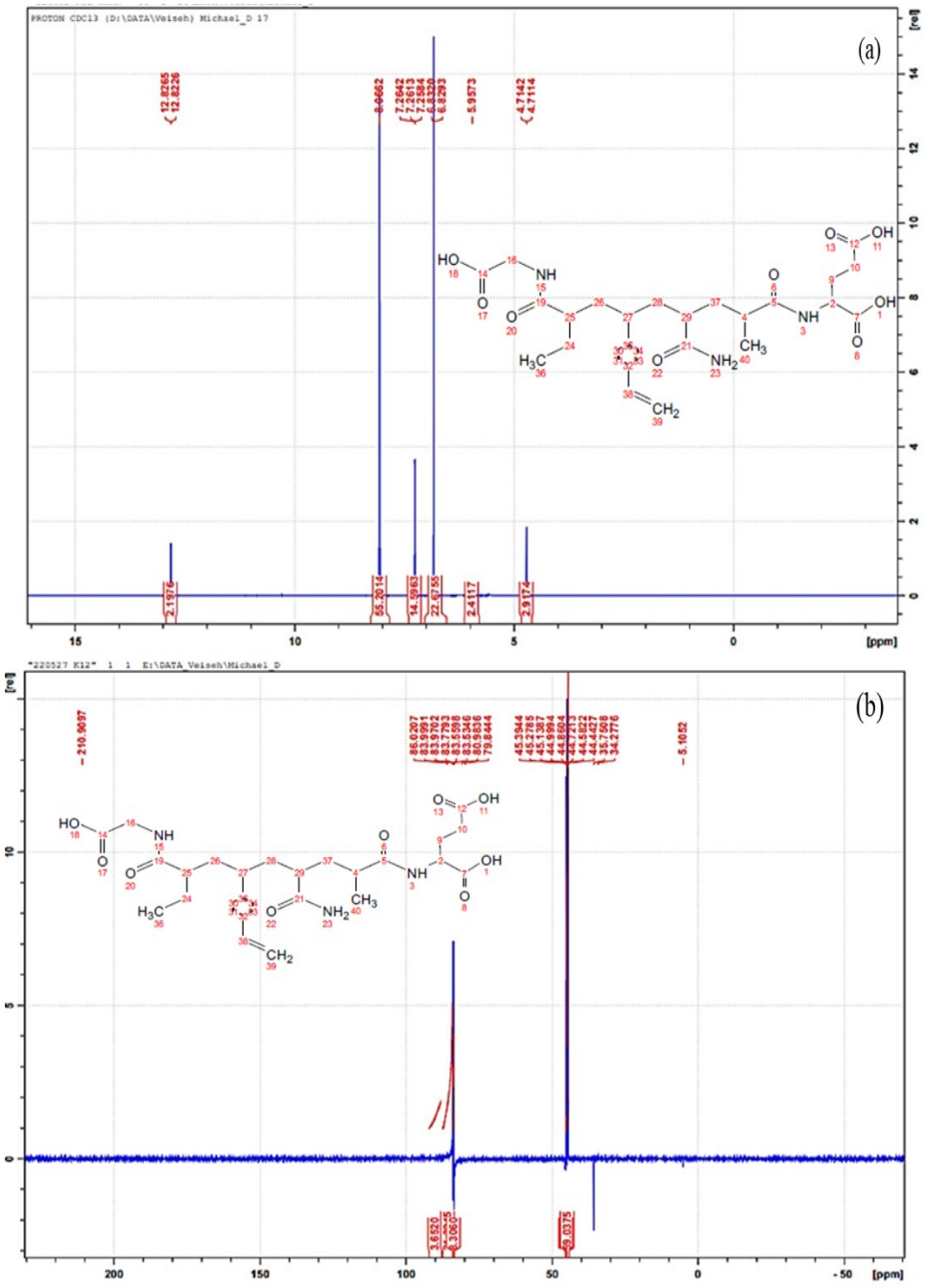

Figure S3. (A) ^{1}H NMR of p(NAG-Ac-NAE) nanohydrogel and (B) ^{13}C NMR of p(NAG-Ac-NAE)) nanohydrogel.

Disappearance and shifting of bands observed in ^{1}H NMR and ^{13}C NMR. For ^{1}H NMR spectrum chemical shifts (in ppm; $CDCl_3$ and DMSO-d_6) (Figure S3(a)): 12.5 δ (O─H of carboxylic acid, 8.9 δ (N─H of 2° amine), 7.26 δ (benzene), compound, 6.8 δ (H_2C ═ CH_2), 6.17 (─CH (12))

^{13}C NMR (500 MHz in ppm; $CDCl_3$ and DMSO-d_6)) (Figure S3(b)): 44 and 34 ppm (8+2 splinted peak of 2° alkane) and 86-79 ppm (carboxylic ─OH and ester)

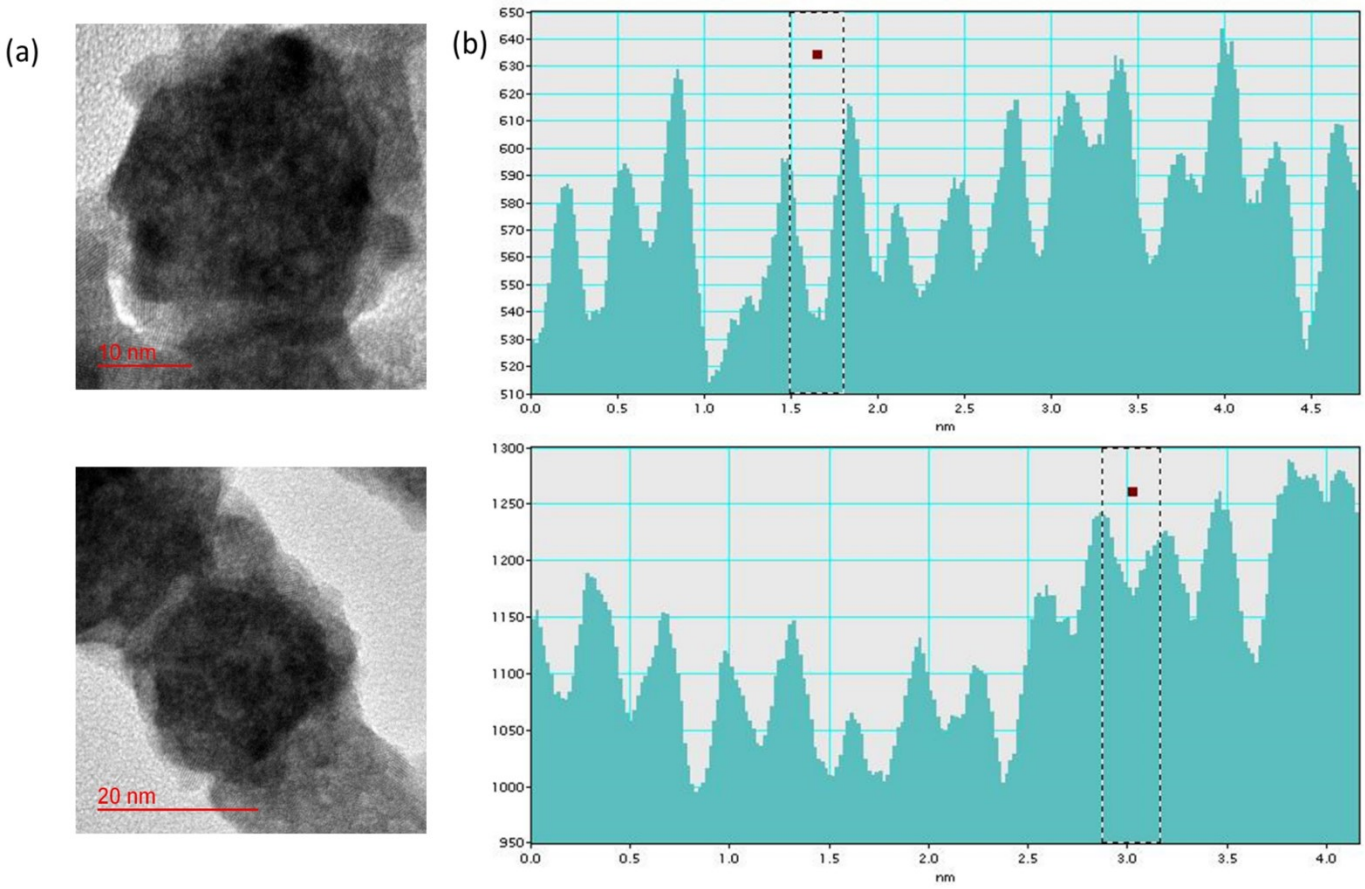

Figure S4. High resolution HRTEM micrograph of p(NAG-Ac-NAE) Hydrogel (a) shows the porous and semi-crystalline nature of the hydrogel particles (b) electron diffraction pattern based distance between two fringes

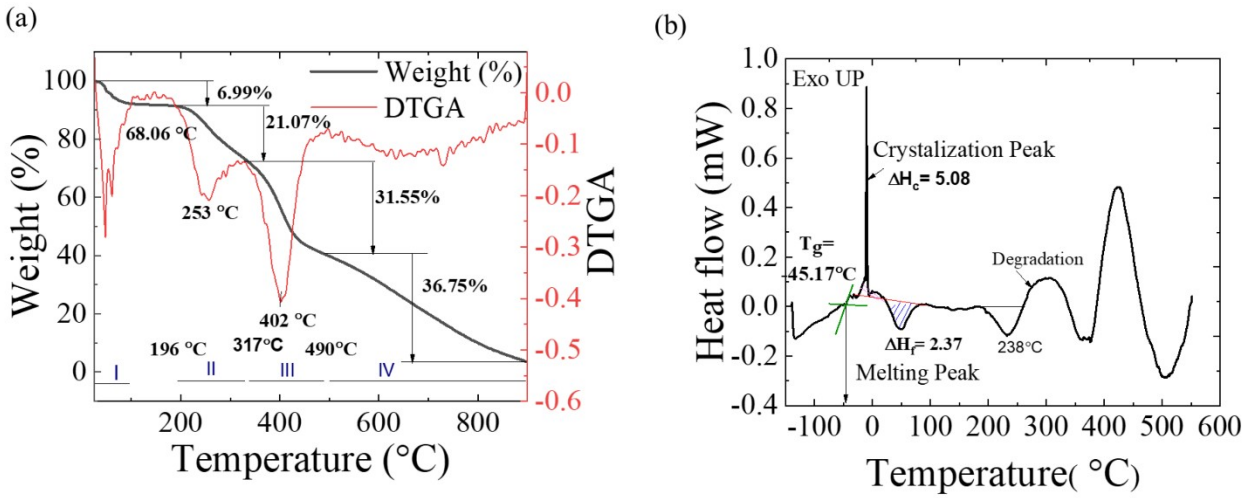

Figure S5. (a) TGA and (b) DSC of the poly(N-acryloylglycine)-co-(acrylamide)-co-(N-acryloylglutamate) hydrogel.

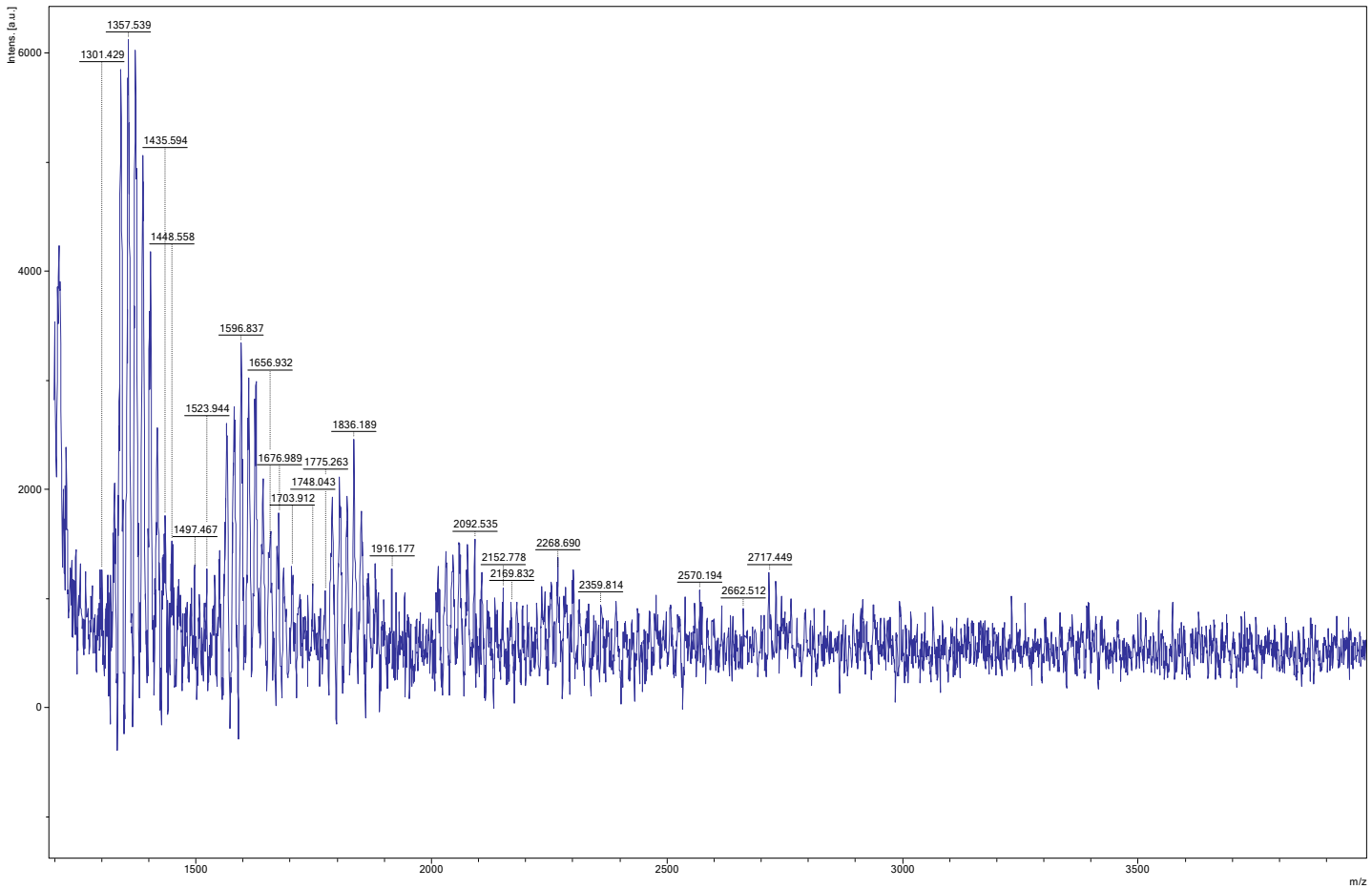

Figure S6. MALDI-TOF spectrum of p(NAG-Ac-NAE) hydrogel

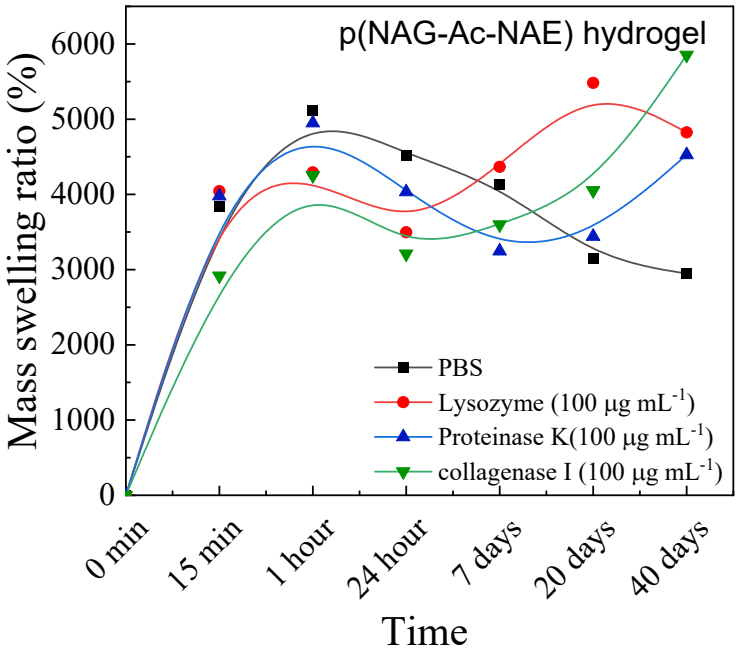

Figure S7. Biodegradation behavior of [p(NAG-Ac-NAE)] without replacing media, studied in PBS (pH 7.4) and in presence of different enzymes.

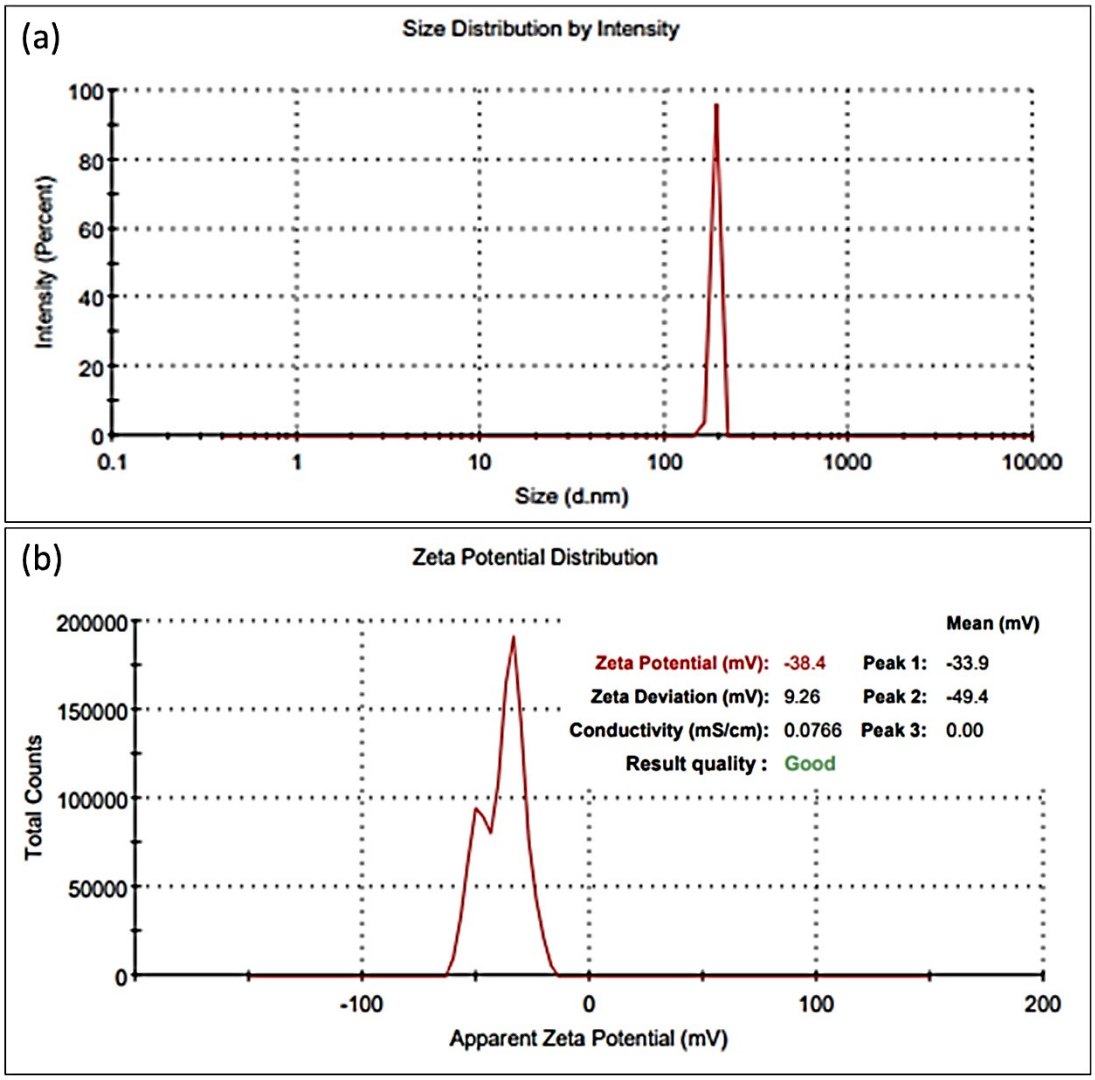

Figure S8. (a) Size distribution and (b) zeta potential of p(NAG-Ac-NAE) hydrogel, studied in PBS (pH 7.4)

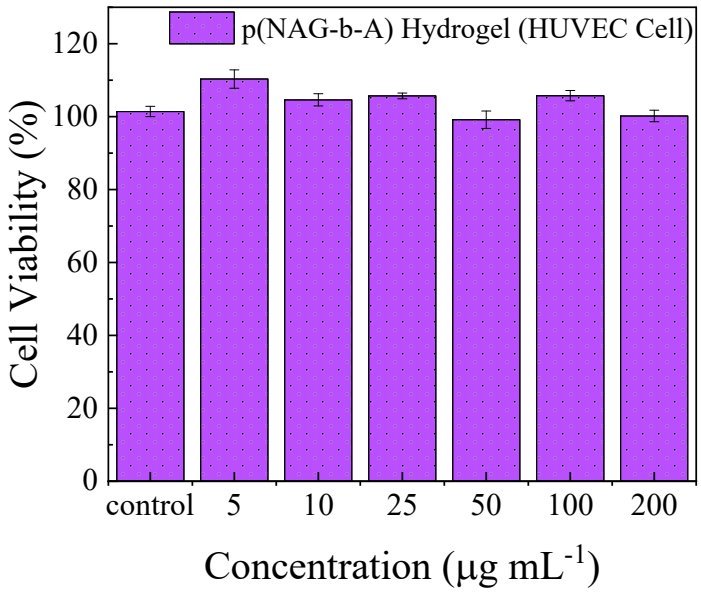

Figure S9. Cell viability of HUVEC cells in treatment of p(NAG-b-A) hydrogel.

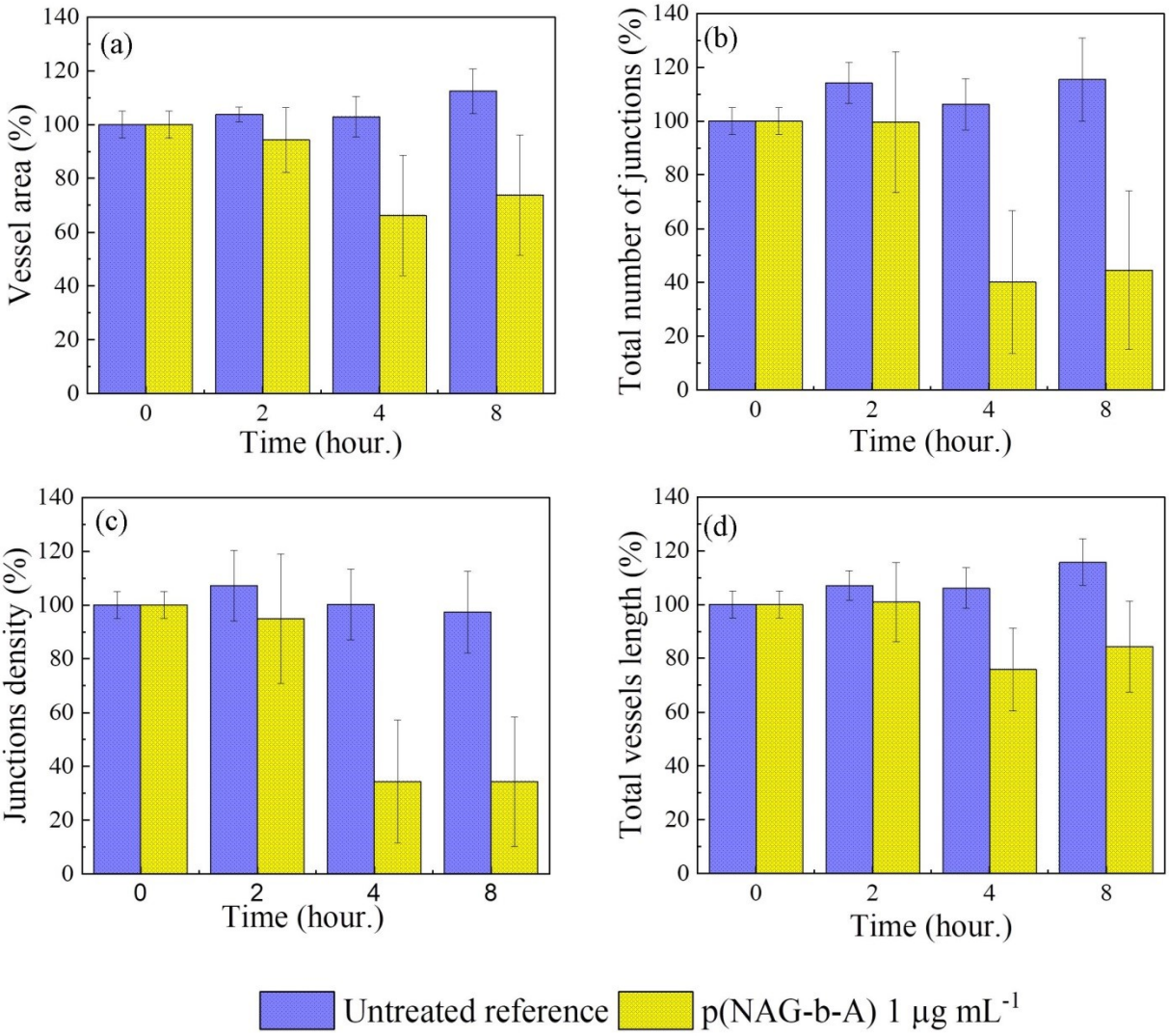

Figure S10. Anti-angiogenic property of p(NAG-b-A) hydrogel. (a) Vessel area (%) vs Time, (b) Total number of junctions (%) vs Time, (c) Junction density (%) vs time and (d) Total Vessel length (%) vs time.

Supporting Information

ABBREVIATIONS:

p(NAG-Ac-NAE), poly (N-Acryloylglycine)-co-(acrylamide)-co-(N-acryloylglutamate) co-polymeric hydrogel; p(NAG-b-A), poly(N-acryloylglycine–b-acrylamide); TNBC, Triple Negative Breast Cancer; CNS, Central Nervous System; PNS, Peripheral Nervous system; TBI, Traumatic brain injury; PLGA, Poly (γ-glutamic acid); AIBN, Azobisisobutyronitrile; DVB, divinylbenzene; FTIR, Fourier transforms infrared; NMR, Nuclear magnetic resonance; HRTEM, High- resolution transmission electron microscopy;XRD, X-Ray Diffraction; TGA, thermogravimetric analysis; DSC, Differential Scanning calorimetry; SAED, Selected area (electron) diffraction; PBS, Phosphate Buffered saline; MCF7, Michigan Cancer Foundation-7;MDA-MB-231, M.D. Anderson - Metastatic Breast 231; PC12, Adrenal phaeochromocytoma; LN229, Glioblastoma cells; AO, acrydin orange; PI, propidium iodide; EtBr, ethidium bromide; NGF, Nerve growth factor; HBSS, Hanks' Balanced Salt Solution; DMEM, Dulbecco's modified Eagle medium; FBS, Fetal bovine serum; MTT, 3-(4,5-dimethylthiazol-2-yl)-2,5-diphenyltetrazolium bromide; BSA, Bovine serum albumin; CEA assay, Chick embryonic assay; NPCs, Neuronal progenitor cells; AD, Alzheimer's disease; PD, Parkinson disease; H_2O_2, Hydrogen peroxide; AKT , three serine/threonine-specific protein kinases; *VEGF, Vascular endothelial growth factor;* PI3K, Phosphoinositide 3-kinases; mTOR, Mammalian target of rapamycin; FESEM, Field emission scanning electron microscopy; G″, Loss modulus; G′, Storage modulus; η*, Complex viscosity; ω, Angular frequency; ANOVA, Analysis of Variance